ANALYTICAL LETTERS
https://doi.org/10.1080/00032719.2023.2262633

Determination of Polystyrene Microplastic in Soil by Pyrolysis – Gas Chromatography – Mass Spectrometry (pyr-GC-MS)

Aline Reis de Carvalho[a], Olivier Mathieu[a], Mathieu Thevenot[a], Philippe Amiotte-Suchet[a], Xavier Bertrand[b], Jean-Charles Beugnot[c], Thomas Karbowiak[d], and Hélène Celle[b]

[a]Biogéosciences, UMR 6282 CNRS, Université de Bourgogne, Dijon, France; [b]Laboratoire Chrono-environnement (LCE), UMR 6249 CNRS-UBFC, Besançon, France; [c]FEMTO-ST Institute, UMR 6174 CNRS-UBFC, Besançon, France; [d]Institut Agro Dijon, PAM, UMR 2102 CNRS-UBFC, Dijon, France

ABSTRACT

Pyrolysis-gas chromatography-mass spectrometry (pyr-GC-MS) is emerging as a promising alternative to the detection and quantification of microplastic pollution. For a robust quantification it is essential to improve our understanding of interferences in the pyrolysis of microplastics. Here we investigate the effects of different soil matrices, mainly differing by their organic carbon content (C_{org}, 1.0–13.6%), and of the polymer Mw on the pyr-GC-MS analysis of polystyrene (PS) microplastics. In addition, we evaluated the effectiveness of adding poly(4-fluorostyrene) (PSF) as internal standard to circumvent the matrix effects. The three main markers of PS pyrolysis, i.e., styrene, styrene-dimer and styrene-trimer, were monitored. The ratio between the dimer and the trimer significantly varied between the matrices and tended to decrease with the increasing of the C_{org} in the soil, mainly due to increased trimer formation. A strong matrix effect affected the slope of the calibration curves by 2 to 8-fold and was correlated with the C_{org} in the soils. This effect was mitigated when the areas of the markers were normalized by the area of the corresponding marker of PSF. PS of low Mw (Mw 35,000) presented a reduced formation of the three markers compared to PS of high Mw (Mw 400,000), and styrene-dimer was proportionally less formed than the other two markers. Differences in the slopes of calibration curves depended on the marker chosen, highlighting the relevance of selecting the pyrolysis marker in the quantification of microplastics using pyr-GC-MS.

ARTICLE HISTORY
Received 29 June 2023
Accepted 20 September 2023

KEYWORDS
Polystyrene microplastic; pyrolysates; pyrolysis – gas chromatography – mass spectrometry (pyr-GC-MS); soil analysis

Introduction

The pervasiveness of microplastic pollution in the environment, i.e., plastic particles smaller than 5 mm, has been followed by an urgent need for analytical methodologies to detect and quantify this pollutant. Soils have been recognized as an important sink of microplastics (Hurley and Nizzetto 2018), which can alter soil physical properties and

CONTACT Aline Reis de Carvalho aline.de-carvalho@u-bourgogne.fr SCT-GOAL, Flemish Institute for Technological Research (VITO), 2400 Mol, Belgium.

Supplemental data for this article can be accessed online at https://doi.org/10.1080/00032719.2023.2262633.

cause decreases in plant height, root biomass, and reproduction rate of soil animals (Zhang et al. 2022). The current methods to detect microplastics in environmental samples mainly focus on extensive protocols to reduce the soil organic and inorganic content to facilitate the microplastic identification (Pinto da Costa et al. 2019; La Nasa et al. 2020; Thomas et al. 2020). Particles are commonly individually analyzed by vibrational spectroscopy (infrared and Raman) (Käppler et al. 2016; Veerasingam et al. 2021) and/or the bulk sample is processed for the detection of microplastics, as in mass spectrometry-based methods (Dierkes et al. 2019; Okoffo et al. 2020; Velimirovic et al. 2021). Vibrational spectroscopy allows the identification of particles composition, their physical properties, such as shape and color, and provides the number of particles in a sample. However, the limit of detection of few micrometers, and the intense sample pretreatment in order to better isolate the particles are considered main disadvantages of these techniques (Renner, Schmidt, and Schram 2018). Thermo-analytical methods, as pyrolysis coupled to gas chromatography and mass spectrometry (pyr-GC-MS), have been emerging as a potential alternative for the analysis of microplastics in complex matrices, such as soils (Peñalver et al. 2020). These methods may shorten the analysis time due to less need of sample clean-up, potentially allowing a direct injection into the equipment with reduced extraction steps (Dümichen et al. 2017; Picó and Barceló 2020; Yakovenko, Carvalho, and ter Halle 2020).

A critical step in pyr-GC-MS is the controlled and reproducible pyrolysis of a sample, which leads to the formation of volatile pyrolysates (Sam 2019). Among these pyrolysates, specific markers of the polymers composing microplastics are sought (Ohtani et al. 1990; Tsuge, Ohtani, and Watanabe 2011). Therefore, the detection of microplastics is performed indirectly, and the presence of one or more markers is extrapolated to the presence of a polymer. The pyrolysis of polystyrene (PS), for instance, mainly generates three markers: the monomer (styrene), the styrene-dimer (3-buten-1,3-diyldibenzene), and the styrene-trimer (5-hexen-1,3,5-triyltribenzene) (Tsuge, Ohtani, and Watanabe 2011; La Nasa et al. 2020). The styrene is commonly the most abundant fragment; however it can also be formed during the pyrolysis of classical soil organic matter constituents, including lignin, and other synthetic polymers, such as polyethylene terephthalate (PET) and acrylonitrile butadiene styrene (Saiz-Jimenez and De Leeuw 1986; Hempfling and Schulten 1990; Dümichen et al. 2015; Dziwiński, Iłowska, and Gniady 2018). Therefore, more specific markers of polystyrene pyrolysis, such as the styrene-dimer and trimer, are usually screened for the presence of polystyrene in pyr-GC-MS analyses.

The quantification of microplastics in environmental samples by pyr-GC-MS is mainly based on external calibration curves, resulting in mass estimates. These curves are established by adding microplastic directly into the pyrolysis system or into a matrix, which usually differs from the one being analyzed (Fischer and Scholz-Böttcher 2017; Ribeiro et al. 2020; Leslie et al. 2022). However, the pyrolysis of microplastics can be strongly affected by a matrix effect, and different slopes between curves have been attributed to an effect of residual mineral components of soil matrices, such as clays (Fabbri, Trombini, and Vassura 1998; Bouzid et al. 2022). In addition, organic components might lead to a variety of volatile pyrolysis products, directly interfering with the specific markers and affecting the quantification of microplastics (Fischer and Scholz-

Böttcher 2017; Picó and Barceló 2020). To overcome the effects of complexes matrices in microplastic quantification, the use of an internal standard (ISTD) is recommended (Unice, Kreider, and Panko 2012), which should ideally mimic the effects suffered by the target analyte during pyr-GC-MS analysis. Different ISTD have been tested, including deuterated polystyrene (PS_{D5}) (Dierkes et al. 2019; Fischer and Scholz-Böttcher 2019; Rødland et al. 2020; Scherer et al. 2020). Recently, extensive matrix-dependent H-D exchanges reactions of PS_{D5} have been demonstrated, and the use of poly(4-fluorostyrene) (PSF) has been preferred (Lauschke et al. 2021). The effectiveness of using PSF as ISTD to increase the accuracy of microplastic quantification in the analysis of complex matrices using pyr-GC-MS remains to be investigated.

The use of calibration curves built with pyrolysis markers of virgin microplastic standards is under the assumption of a similar pyrolytic behavior between this reference material and the microplastic in the environment. However, changes in the molecular structure of the microplastic, such as appearance of carbonyl groups due to an oxidation process, are shown to affect the formation of its markers during pyrolysis (Ainali, Bikiaris, and Lambropoulou 2021a; Toapanta et al. 2021). Moreover, polymer molecular weights (Mw) have already been highlighted as an important determinant of pyrolysis yields (Audisio and Bertini 1992; Guo et al. 2017; Park and Lee 2021). Styrene yield, for instance, was shown to increase with the Mw of polystyrene (Bouster, Vermande, and Veron 1989). In addition, microplastics might present diverse patterns of Mw distribution (ter Halle et al. 2017), likely differing from the virgin polymers used to build calibration curves. For reliable estimates of microplastic in environmental samples, it is crucial to understand the effect of Mw on pyr-GC-MS analysis and the consequences on microplastic quantification.

In this study, we aim to investigate the effects of the matrix and the polymer Mw on the PS quantification using pyr-GC-MS. First, we assess the effect of different soil matrices, mainly differentiated by their organic carbon content, on the pyrolysis of PS. Then, we verify the effectiveness of PSF as an internal standard to circumvent matrix effects. Second, we compare the pyrolysate yields from PS of two different Mw and we evaluate the effect on the quantification of this microplastic. Specifically, we investigate the changes in the proportion of the main PS markers and the effect on the slope of calibration curves.

Methodology

Standards acquisition

Polystyrene microplastics of low Mw (PSLMW, average Mw 35,000, Merck KGaA, Darmstadt, Germany, 331651, CAS: 9003-53-6) were obtained as pellets and ground in a microfine grinder (MF10, IKA-Werke GmbH & Co. KG, Germany) at 3000 rpm using a 1.0 mm sieve. The collected powder was successively sieved through 500, 200, 100, and 63 µm mesh sieves. Polystyrene microplastics of high Mw (PSHMW, average Mw 400,000) were purchased as a powder with an average particle size of 300 µm (Merck KGaA, Darmstadt, Germany, 450383, CAS: 9003-53-6). Poly (4-fluorostyrene) (PSF, average Mw 3,200) was purchased from Polymer Source as the powder (Montreal, Canada, P43491A).

PSF and PSLMW were dissolved in dichloromethane (Sigma Aldrich, 34856, CAS: 75-09-2) to prepare a solution at 200 µg mL^{-1}. PSHMW was insoluble in the solvents tested (dichloromethane, chloroform, toluene, and ethyl acetate), and no solution could be prepared.

Matrices analyzed

Acid-washed sand, SiO_2, (Fisher Chemical, S/0330/65, CAS: 14808-60-7) was heated at 600 °C in a porcelain grail overnight prior to use. Then, the sand (SA) was ground in the Mixer Mill (Retsch MM400) under 20 Hz for 3 min using a single 20 mm diameter zirconium ball. Sand was composed only of sandy texture (1000 mg g^{-1}), and its carbon organic content was considered as null.

Five soils were obtained from a previous work by Guigue et al. 2014, along with their parameters of organic carbon content (Corg, ranging from 10 mg g^{-1} to 136 mg g^{-1}, i.e., 1.0–13.6% (w/w)) and other characteristics, such as nitrogen content, carbon/nitrogen ratio, texture and pH. These soils are developed on different source materials, with various vegetation types and cover a wide spectrum of organic matter composition and concentration. Briefly, for each soil, a 5 kg composite of the A-horizon was collected from a soil pit with well-defined horizons. All soils were air-dried, sieved through a 2 mm mesh, and homogenized before further experiments. GL is a Gleyic Luvisol (Corg = 10 mg g^{-1}) collected from an agricultural area in the Burgundy region (47°07′23″N; 5°05′08″E), presenting a massive structure and was bare at the time of sampling. EC is an Eutric Cambisol (Corg = 25 mg g^{-1}) collected in the Burgundy region (47°23′12″N; 4°39′19″E), at the bottom of a valley, at calcareous alluvial deposits surrounded by carbonate rocks. DC is a Dystric Cambisol (Corg = 30 mg g^{-1}) collected in the Burgundy region (47°06′16″N; 4°25′55″E), with vegetation composed mainly of gramineous pasture. EP is an Entic Podzol ($C = 66$ mg g^{-1}) collected in the Franche-Comté region (47°11′29″N; 5°33′50″E), well-drained and with the presence of a thick, acidic mor-type organic horizon. DA is a dystric Andosol (Corg = 136 mg g^{-1}) collected in the Auvergne region (45°40′37″N; 2°57′53″E), an organic-rich soil characterized by a low bulk density and the presence of allophanes (Guigue et al. 2014).

Sample preparation and analysis by pyr-GC-MS

PSLMW solution in the presence or absence of matrices

Calibration curves of PSLMW solution (in dichloromethane, 200 µg mL^{-1}) were prepared by adding 5 to 25 µL of solution, corresponding to 1 to 5 µg of PSLMW, in pyrolysis cups (Eco-Cup LF, PY1-EC80F, Frontier Lab) already containing 10 µL of PSF (in dichloromethane, 200 µg mL^{-1}), which was used as an internal standard (ISTD). The pyr-cups were taken under the fume hood at room temperature for 15 min to allow the solvent to evaporate. A total of seven curves were built, with and without the addition of 5 mg of each matrix analyzed, already milled in the Mixer Mill (SA, GL, EC, DC, EP, DA, displayed in the increasing order of Corg). Procedure blanks consisted of the matrix without the addition of PSLMW solution and submitted to the same sample procedure.

Matrices spiked with PSLMW and PSHMW powder

To build calibration curves, a first sample (solution A) was prepared by the addition of 40 mg of each type of PS, individually, into 4 g of matrix to a final concentration of 10 g kg^{-1}. The SA matrix was used for PSLMW (200 – 500 µm fraction), while GL, EC, DC, EP and DA were used for PSHMW. This content was mixed and ground in the mixer mill. Then, a fraction was weighed (Sartorius, SECURE 225D-15, readability = 0.01 mg) and spiked into a matrix to prepare solutions of 1.25, 1.00, and 0.50 g kg^{-1}. From these secondary samples, a fraction was weighed to prepare samples of 0.25, 0.10, and 0.05 g kg^{-1}, respectively. Finally, each sample was ground by the mixer mill. The final concentrations were calculated considering the weight of sample added and the weight of blank matrix, resulting in small variations in the concentrations at the same calibration level. Procedure blanks consisted of the matrix without the addition of PS and submitted to the same sample procedure.

Approximately 5 mg of each sample with a concentration of 0.05 to 1.25 g kg^{-1} and procedure blanks were weighed in a microbalance (Sartorius, CUBIS MSU 6.6S, readability = 0.001 mg) directly into a pyr-cup. The value was recorded for the nearest 0.001 mg. The amount of injected polymer was calculated by the mass of the sample and its concentration. When indicated, this final step was repeated, and it is displayed as replicate.

Contamination control

To avoid any contamination during the sample preparation procedure, nitrile gloves and cotton lab coats were always worn. The working surface was cleaned with ethanol and deionized water before each procedure, and glassware and metalware were used whenever possible, also rinsed with deionized water before their use. All steps during the procedure were preferably performed under a fume-hood, and sample containers were always covered with aluminum foil to avoid airborne contamination. All pyrolysis cups for pyr-GC-MS were heated at 600 °C in a porcelain grail overnight prior to use. Procedural blanks, composed only by the matrix under study, were submitted to the same procedure as the samples and were further analyzed to check for the presence of sources of contamination.

Pyr-GC-MS analysis

Samples in pyr-cups were covered with quartz wool (ThermoFisher, 33822200, CAS: 60676-86-0,) and then analyzed by pyrolysis (EGA/Py 3030D, autosampler, FrontierLab) – gas chromatography (GC 7890, Agilent Technologies, Santa Clara, CA USA) – mass spectrometry (MSD 5978B, Agilent Technologies, Santa Clara, CA USA). Pyrolysis was performed at 600 °C for 30 s under helium, followed by a chromatographic separation in an Ultra-Alloy+ – 5 column (30 m × 0.25 mm × 0.25 µm, Frontier Lab), with helium as a carrier gas and oven program at 40 °C for 2 min, 20 °C min^{-1} until 320 °C and hold for 6 min. An interface temperature of 300 °C, split of 1:20 and a constant flow of 1 mL min^{-1} were settled. The molecules were ionized at the source (EI, 70 eV, 230 °C) and the quadrupole analysis included the full scan (from m/z 45 to 600) and SIM modes. The most intense m/z of the main compounds originated from the

Table 1. Markers obtained from the pyr-GC-MS analysis of polystyrene low molecular weight (PSLMW), polystyrene high molecular weight (PSHMW) and poly (4-fluorostyrene) (PSF), and their respective m/z monitored in single ion monitor (SIM) mode and Kovats' retention indices (RI).

Compound	Polymer	m/z	RI
Styrene (monomer)	PSLMW or PSHMW	104	902
3-buten-1,3-diyldibenzene (dimer)		91	1741
5-hexen-1,3,5-triyltribenzene (trimer)		91	2496
4-Fluorostyrene (styrene-F)	PSF	122	908
2,4-di(4-fluorophenyl)but-1-ene (dimer-F_2)		109	1749
2,4,6-tri(4-fluorophenyl)hex-1-ene (trimer-F_3)		109	2470

pyrolysis of PSLMW/PSHMW or PSF was monitored (Table 1). The retention time for each compound was defined by the injection of PSLMW and PSF solution and the spectra comparison with the literature (Tsuge, Ohtani, and Watanabe 2011) and with the NIST 14 library (v. 2.3). Kovats' Retention indices (RI) were calculated using the retention times of the n-alkanes determined in the pyrogram of polyethylene under the same pyr-GC-MS conditions (IUPAC 1997).

Data analysis and visualization

The data from peak integration was obtained with the MassHunter Workstation software (v. B.07.00, Agilent Technologies, Santa Clara, CA USA) and the data analyses were performed at R v.4.2.2 (R Core Team 2022).

The procedural blanks and the instrumental blanks (empty cups) were analyzed to check the presence of the target compounds. Procedural blanks were analyzed in the same sequence of the respective samples, and instrumental blanks were injected at every injection of 5 samples. No peaks of the target compounds were detected in the blanks, except for the styrene in soil samples, indicating that no contamination occurred during sample handling.

The surface area obtained for each marker of PS pyrolysis was always corrected by the weight of sample to obtain the corrected mass of polymer injected in each analysis. Therefore, small variations in calibration levels are expected, without affecting the purposes of this study. Linear regression models were applied to test the relationship between the mass of the polymer and the surface area of the markers. Analysis of variance (ANOVA) tests (stats package v 4.1.2, R Core Team 2022) were computed to estimate the effects of matrix or polymer Mw and the injected polymer mass, or their interaction, on the area of markers, always carried out within a marker type, once different markers are expected to have different responses. In the presence of a significant interaction, post-hoc pairwise comparison tests were performed with emmeans function (emmeans package, v 1.7.2, Lenth et al. 2023).

To analyze changes in the formation rate of pyrolysates against different matrices or polymer Mw, two indicators were explored. The first consisted of the percentage of styrene monomer (Equation 1); dimer or trimer and was applied for samples without matrix or in the presence of sand. In the presence of soils, and therefore of styrene naturally originated from the pyrolysis of these matrices, the formation of dimer and trimer was explored by their ratio (dimer/trimer, or $R_{D/T}$). In the absence of styrene-dimer signal (low PS concentrations), the ratio was not calculated. Peak area ratios can

be compared between different samples to allow the identification of different pyrolysis pattern.

$$Styrene\ (\%) = \frac{Area\ \ styrene}{(Area\ \ styrene + Area\ \ dimer + Area\ \ trimer)} * 100$$

Equation 1. Calculation of the relative percentage of styrene against the three main markers

Differences on these indicators were tested by Wilcoxon or Kruskal-Wallis tests (stats package, R Core Team 2022). If the Kruskal–Wallis test was significant ($p < 0.05$), a post-hoc analysis was performed to determine which levels differed from each other by Dunn test (FSA package, v 0.9.3, Ogle, Doll, and Wheeler 2023). Significant differences between these indicators, i.e., $p < 0.05$, among different matrices or polymer types are indicated in each plot as different letters.

Correlations between the Corg and the (i) $R_{D/T}$ and (ii) the slope of calibration curves were tested using Spearman correlation tests (stats package). Before testing the correlation between the other soil parameters, i.e., nitrogen content and soil texture (sand, loam, and clay composition, Table S1), and (i) and (ii), we tested the correlation among soil parameters. The Corg was strongly and positively correlated with nitrogen content ($\rho = 0.99$, $p < 0.01$), and the sand content was negatively correlated with the loam content ($\rho = -0.94$, $p < 0.01$). Therefore, sand and clay compositions were the soil parameters further used to test the correlation with (i) and (ii).

For the study of the effectiveness of ISTD, the surface area obtained for each marker of PSF pyrolysis, i.e., styrene-F, dimer-F_2 and trimer-F_3, was used to normalize the surface area of the equivalent marker of PS, i.e., styrene, dimer and trimer. To analyses changes in the formation of PFS pyrolysates, the percentage of styrene-F and the ratio dimer-F_2/trimer-F_3 ($R_{DF2/TF3}$) were calculated.

The data were plotted using ggplot2 package v 3.3.5 (Wickham et al. 2023). In boxplots, the lower and upper hinges correspond to the first and third quartiles. The upper whisker extends from the hinge to the largest value no further than 1.5 * IQR from the hinge (where IQR is the inter-quartile range, or distance between the first and third quartiles). In linear plots, the symbols represent the actual values, and the lines represent the fitted trend, while shadows around the curve represent the 95% confidence interval.

Results

Effect of matrix upon the pyrolysis of PSLMW

In the procedural blanks, no PS markers were detected for the SA matrix. For blank soil matrices, a peak of styrene was noticed (Figure S1a) and their surface areas were strongly correlated with the Corg of the matrices (Spearman, $\rho = 0.99$, $p < 0.01$) (Figure S1b).

Pyr-cups spiked with PSLMW solution in the presence or absence of matrices were analyzed to evaluate their effect on the pyrolysis of this polymer. In the absence of matrix, the styrene was the major pyrolysate of PSLMW, accounting for 94.5% (± 0.5) of the three markers, followed by the trimer (3.8 ± 0.5) and the dimer (1.7 ± 0.1) ($n = 5$). The same profile was observed with the addition of matrix; however, the percentage of each marker significantly varied between the matrices (Kruskal-Wallis, $p < 0.01$). The

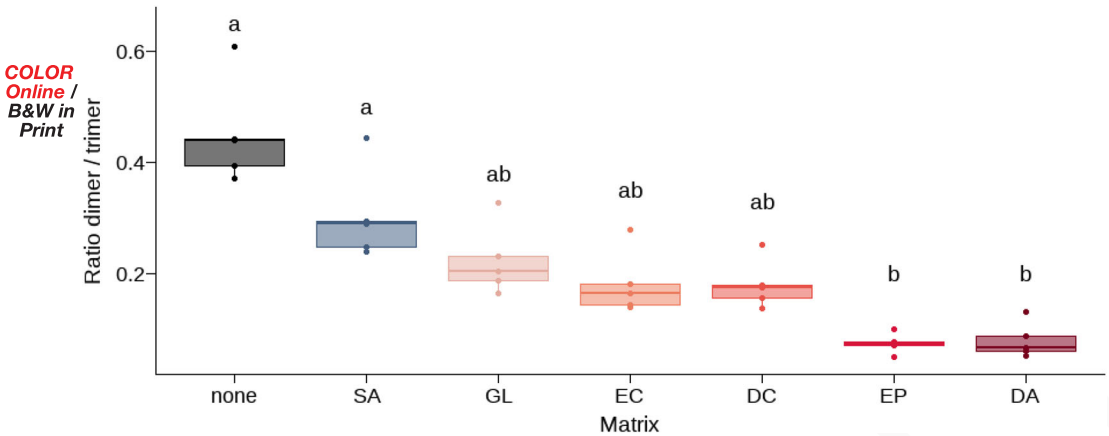

Figure 1. Ratio ofdimer/trimer ($R_{D/T}$) from pyr-GC-MS analysis of polystyrene low molecular weight (PSLMW) without or with the presence of matrices (sand (SA), gleyic luvisol (GL), eutric cambisol (EC), dystric cambisol (DC), entic podzol (EP), dystric andosol (DA), $n = 5$). Darker red represents matrices with higher organic carbon content. Different letters indicate significant differences ($p < 0.05$).

styrene accounted for 88.8% (± 1.0), on average, of the three markers for the DA matrix, while the trimer represented 10.3% (± 1.2) (Table S1). No correlation was found between the areas of the three markers. The trimer areas were significantly and positively correlated with the Corg of matrices (Spearman test, $\rho = 0.99$, $p < 0.01$). No other significant correlation was found between the marker's areas and the soils parameters.

The $R_{D/T}$ formed during the pyrolysis of PSLMW varied significantly in the presence of different matrices (Figure 1) and were negatively correlated with the Corg of matrices (Spearman test, $\rho = -0.86$, $p < 0.01$), notably due to the increased formation of trimer. No significant correlation was found between the $R_{D/T}$ and the contents of sand and clay in the soils (Spearman test, $p > 0.05$). The differences among matrix types were significant, even though a variation in the $R_{D/T}$ with different amounts of polystyrene pyrolyzed was noticed within each matrix. The outlier ratio value in the upper whisker within each matrix (Figure 1) corresponds to the smallest injected mass of PSLMW, i.e., 1 µg, demonstrating the existence of an optimal range for analytical detection.

Calibration curves built with each marker presented an overall good linearity (R^2 greater than 0.88, Figure 2 and Table S2). Thus, the presence of the matrix had a significant and distinct effect on the response of styrene-dimer and trimer to the pyrolysis of PSLMW (ANOVA, $p < 0.01$) (Figure 2). In the presence of a matrix, the curves for the styrene-dimer were up to 3-fold less steep (Figure 2a), indicating reduced formation of this marker. For the styrene-trimer, the differences in slopes were up to 4-fold and matrix-dependent (Figure 2b), positively and strongly correlated with the Corg of matrices (Spearman test, $\rho = 1.0$, $p < 0.01$). The only significant correlation between the slopes and the other soil characteristics was found for the slopes of dimer curves and the sand content (Spearman test, $\rho = 0.6$, $p < 0.01$).

Attenuation of matrix effect using ISTD

Pyr-cups spiked with PSF solution in the presence of absence of matrices were analyzed to evaluate the pyrolysis of this polymer. The formation of the three main markers of

COLOR Online / B&W in Print

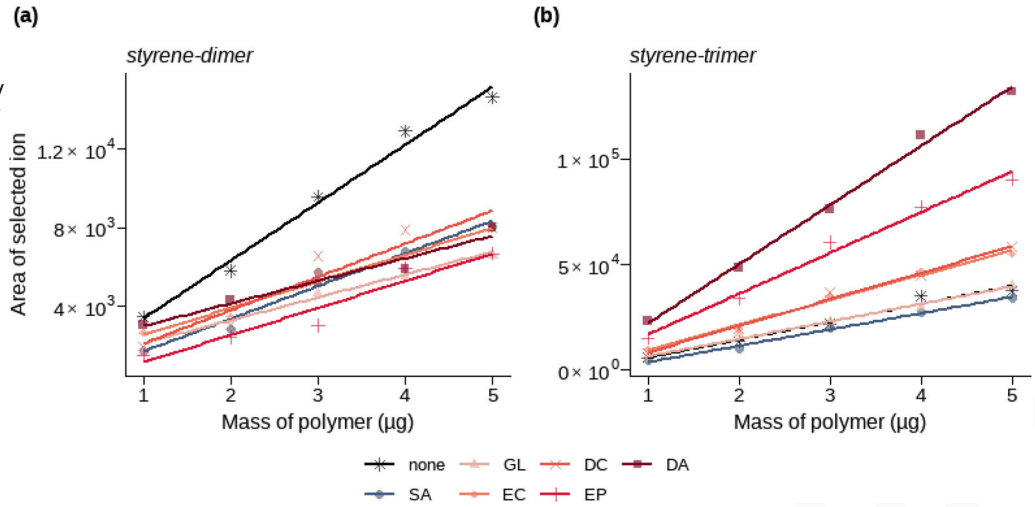

Figure 2. Calibration curves of polystyrene markers (a) styrene-dimer and (b) styrene-trimer from polystyrene low molecular weight (PSLMW) solution in the absence or presence of matrix (sand (SA), gleyic luvisol (GL), eutric cambisol (EC), dystric cambisol (DC), entic podzol (EP), and dystric andosol (DA). Darker red represents matrices with higher organic carbon content.

Table 2. Peak area of the three main poly (4-fluorostyrene) (PSF) markers formed during the pyr-GC-MS analysis in the absence or presence of matrix (sand (SA), gleyic luvisol (GL), eutric cambisol (EC), dystric cambisol (DC), entic podzol (EP), and dystric andosol (DA), $n = 5$).

Matrix	Average Styrene-F ± SD ($\times 10^6$)	Average Dimer-F_2 ± SD ($\times 10^4$)	Average Trimer-F_3 ± SD ($\times 10^4$)	Average ratio dimer-F_2/trimer-F_3 ± SD
None	1.23 ± 0.10	6.17 ± 0.34	7.24 ± 0.87	0.86 ± 0.10
SA	1.13 ± 0.12	3.72 ± 0.27	6.04 ± 0.61	0.62 ± 0.05
GL	1.29 ± 0.03	3.32 ± 0.28	8.54 ± 1.59	0.40 ± 0.05
EC	1.30 ± 0.06	3.40 ± 0.30	12.0 ± 0.86	0.28 ± 0.02
DC	1.33 ± 0.13	3.30 ± 0.80	13.4 ± 1.24	0.24 ± 0.05
EP	1.70 ± 0.08	2.86 ± 0.51	20.7 ± 1.15	0.14 ± 0.03
DA	1.66 ± 0.05	3.01 ± 0.19	29.2 ± 0.99	0.10 ± 0.01

PSF pyrolysis was strongly impacted by the presence of the matrix (Kruskal-Wallis, $p < 0.01$), as it was observed for the pyrolysis of PSLMW. Dimer-F_2 was gradually less formed from the SA to DA matrix, while the opposite profile was observed for the styrene-F and trimer-F_3 (Table 2). The formation of styrene-F and trimer-F_3 was strongly and positively correlated with the Corg of matrices (Spearman, $\rho = 0.80$ and $\rho = 0.96$, respectively, $p < 0.01$). No correlation was found between the areas of styrene-F and dimer-F_2, while the former was positively correlated with trimer-F_3 areas (Spearman, $\rho = 0.79$, $p > 0.01$). No other significant correlation was found between the marker's formation and other soils parameters.

The $R_{DF2/TF3}$ from PSF pyrolysis (Figure S2) showed a behavior similar to the $R_{D/T}$ from PSLMW in the presence of different matrices (Figure 1), and were also negatively and strongly correlated with Corg of matrices (Spearman, $\rho = -0.97$, $p < 0.01$). No other significant and strong correlation was found between the $R_{DF2/TF3}$ and other soils parameters. As for the PSLMW case, the decreasing $R_{DF2/TF3}$ from SA to DA matrix was mainly attributed to the increased formation of the trimer.

COLOR Online / B&W in Print

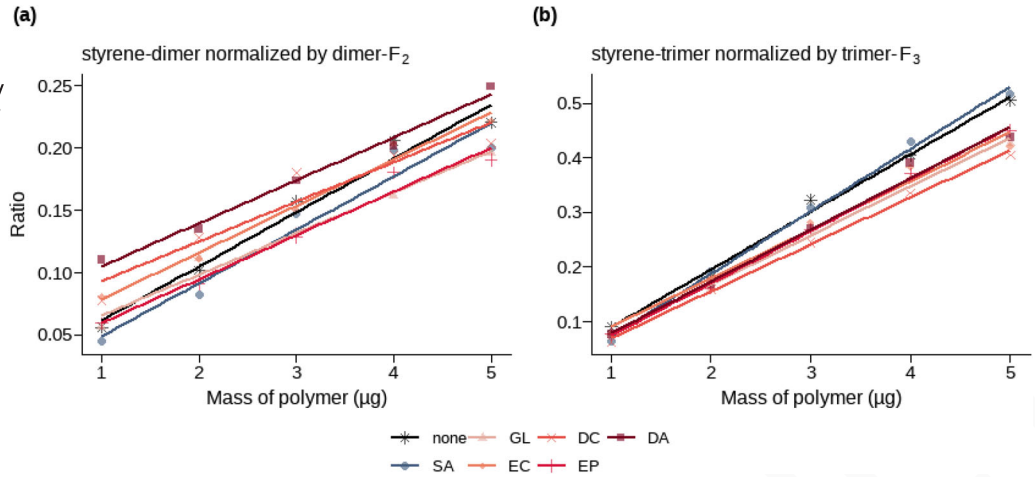

Figure 3. Calibration curves of polystyrene markers (a) styrene-dimer (normalized by dimer-F_2) and (b) styrene-trimer (normalized by trimer-F_3) from pyr-GC-MS analysis of polystyrene low molecular weight (PSLMW) solution in the presence of different matrices (sand (SA), gleyic luvisol (GL), eutric cambisol (EC), dystric cambisol (DC), entic podzol (EP), dystric andosol (DA)). Darker red represents matrices with higher organic carbon content.

Using the monomer styrene-F to normalize the surface areas of styrene-dimer and trimer did not circumvent the matrix effect (Figure S3a and b, respectively). On the other hand, normalization of styrene-dimer by dimer-F_2 eliminated the matrix effect for styrene-dimer, i.e., the differences in the slopes of the curves (Figure 3a). For the styrene-trimer curves, normalization of styrene-trimer by trimer-F_3 significantly reduced the difference between the slopes to 1.3 fold, although a significant interaction between them and the matrix type was still present (ANOVA, $p < 0.01$, Figure 3b). In most cases, the normalization by the ISTD improved the fit of linear models (R^2) of the calibration curves (Table S2).

Effect of polymer Mw on the pyrolysis of PS

For the comparison between the pyrolysis of PSLMW and PSHMW, sand spiked with the respective microplastic powder was used. In general, the signal of PS markers in the pyrolysis of PSLMW was always less intense than those of PSHMW for the same amount of microplastic spiked in sand (Figure S4). Considering the three markers, styrene is proportionally more formed for PSLMW than for PSHMW (Table 3, Wilcoxon test, $p < 0.01$). Conversely, more styrene-dimer was formed for PSHMW than for PSLMW (Table 3, Wilcoxon test, $p < 0.01$), whereas no significant difference was observed in the formation of styrene-trimer (Table 3). The $R_{D/T}$ was significantly greater for PSHMW (Wilcoxon test, $p < 0.01$, Table 3), notably due to the favored formation of dimer.

Calibration curves were built with the three markers obtained from PSHMW or PSLMW spiked in sand (R^2 bigger than 0.78, Figure 4 and Tables S4 and S5). All three markers were detected in the smallest concentration for PSHMW, i.e., 0.05 g kg^{-1}, but the styrene-dimer was only detected in one of the replicates. The styrene-dimer was

Table 3. Proportion of the three main polystyrene markers formed during the pyr-GC-MS analyses of polystyrene low molecular weight (PSLMW) or polystyrene high molecular weight (PSHMW) spiked in sand (averaged ± standard deviation, SD).

Polymer	Average of styrene (%) ± SD (*)	Average of dimer (%) ± SD (*)	Average of trimer (%) ± SD	Ratio dimer / trimer ± SD (*)
PSHMW ($n = 12$)	94.14 ± 1.73	3.59 ± 1.16	2.27 ± 0.67	1.60 ± 0.37
PSLMW ($n = 9$)	96.72 ± 0.98	1.29 ± 0.40	2.00 ± 0.63	0.65 ± 0.13

Significant differences ($p < 0.05$) are displayed with an asterisk.

COLOR Online / B&W in Print

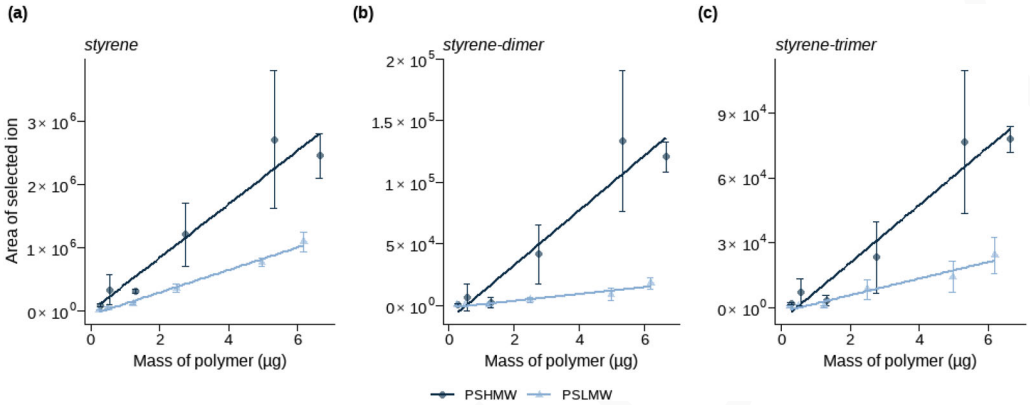

Figure 4. Calibration curves of polystyrene markers (a) styrene, (b) styrene-dimer and (c) styrene-trimer from pyr-GC-MS analyses of polystyrene high molecular weight (PSHMW) (dark blue) and polystyrene low molecular weight (PSLMW) (light blue) spiked in sand ($n = 3$).

only consistently detected when the concentration was greater than 0.25 g kg^{-1}, equivalent to 1.25 µg of polymer (Table S3). The average RSD for styrene areas were higher for PSHMW than PSLMW (35.3% and 19.8%, respectively); however the opposite was noticed for the dimer and trimer (36.9% and 52.6% for PSHMW and 42.8% and 84.9% for PSLMW) (Table S3). The highest relative standard deviation of slopes was found for the curves of trimer from PSLMW (RSD 32.1%, $n = 3$, Table S3). The slopes of the curves differed significantly among PS types for all markers (ANOVA, $p < 0.01$, Figure 4) from 2 to 8-fold, with the greatest variation for the styrene-dimer (Figure 4b). Using the linear equation obtained from PSHMW to estimate the PS concentration in a sample containing PSLMW lead to underestimates in a 2.5 to 5.3-fold range, depending on the marker chosen (Table S5).

Analysis of soils spiked with PSHMW

For PSHMW microplastic powder spiked in different matrices and submitted to a milling process, the $R_{D/T}$ significantly differed between matrix types (Kruskal-Wallis test, $p < 0.01$, Figure S5), following the same profile as previously described for PSLMW and PSF solutions (Figure 1 and Figure S2, respectively). The $R_{D/T}$ from PSHMW were also negatively correlated with the Corg in soils (Spearman, $\rho = -0.85$, $p < 0.01$). Compared to the $R_{D/T}$ from PSLMW, those from PSHMW were overall higher, notably due to the higher amount of dimer being formed in the pyrolysis of PSHMW. The $R_{D/T}$ from

PSHMW were not correlated with the sand and clay content of the matrices (Spearman, $p > 0.05$).

Calibration curves were built from the pyrolysis of PSHMW powder spiked in different matrices (R^2 greater than 0.75, Table S4). Both markers, dimer and trimer, were detected in the lowest concentration, i.e., 0.05 g kg^{-1}, only in SA. For all the soil matrices, these markers were only detected in concentrations above 0.10 g kg^{-1}, equivalent to 0.5 µg of polymer. The slopes of curves built with the styrene-dimer varied significantly with matrix type by about 3.0-fold. Specifically, the slope of the curve in GL was significantly smaller than DC, EP and SA (emmeans, $p < 0.01$, Figure S6a). For the trimer, the slopes of curves showed a larger variation up to 7.5-fold (Figure S6b), and GL soil presented a significantly steeper curve than DA, EP, and EC (emmeans, $p < 0.01$). The slopes of curves built with the trimer were positively and strongly correlated with the Corg of matrices (Spearman test, $\rho = 0.88$, $p < 0.01$), similarly as observed for the curves built with this marker from PSLMW. No significant correlation was found between the slopes and the contents of sand and clay in the matrices (Spearman test, $p > 0.05$).

Discussion

We demonstrate in this work that the pyr-GC-MS analysis of PS is affected by external and internal factors interfering with the formation of its main markers. The first is a matrix effect, which affected the formation rate of markers and the slope of the calibration curves, and was circumvented by the normalization with PSF. The second, the polymer Mw, which directly affected the pyrolysates yields of PS and the slope of the calibration curves, leading to estimate errors in microplastic concentration.

Pyr-GC-MS analysis of PS microplastics, one of the most commonly used materials and largely found in the soil environment as debris (PlasticsEurope 2020; Huang et al. 2021), was strongly affected by the presence of matrices. Previous studies have shown an increased background in pyrograms with organic-rich soils (up to 5.6% Corg) mainly due to the detection of a PS marker, styrene, originating, for instance, from chitin or phenylalanine content (Fischer and Scholz-Böttcher 2017; Steinmetz et al. 2020). Here we showed that the Corg of soils was indeed strongly correlated with their styrene content naturally present, and none of the two other PS markers was detected. With the addition of PS in different matrices, the formation of its markers significantly differed, notably with a higher formation of trimer with the increasing Corg. A similar behavior was noticed during PSF pyrolysis, with higher formation of trimer-F_3 with the increasing Corg in matrices, highlighting the existence of matrix effect likely related to the Corg. The higher yield of trimer might be a consequence of reduced secondary reactions, preventing the conversion of trimer to dimer and/or monomer (Zhou et al. 2016), and here correlated to the greater presence of other organic compounds. Though the constituents of these soils were not fully characterized, no other significant or strong correlation was found between the other matrix parameters and the formation of markers. The presence of inorganic constituents, or their interaction with the organic ones, might also interfere in the PS pyrolysis (Fabbri, Trombini, and Vassura 1998; Bu et al. 2017). For instance, the adsorptive effect of clay materials was showed to cause a reduced detection of all PS markers (Fabbri, Trombini, and Vassura 1998; Bouzid et al.

2022). Clays might exhibit either a catalysis or a pyrolysis-inhibiting effect during pyrolysis, depending on the nature of the organic compound and of the clay-organic matter complex (Bu et al. 2017; Zhou, Yang, and Wang 2017). No correlation was found between the amount of clay in the soils and the formation of pyrolysis markers; however, the different natures of clay might play a role in the pyrolysis yields of microplastics (Faure et al. 2006). Further studies are necessary to fully elucidate the matrix components that interfere in the formation of polystyrene markers during the pyr-GC-MS analysis and how they might affect the pyrolysis of other microplastic types.

We add evidence that the use of external calibration curves built in distinct matrices for the quantification of microplastic lead to great errors (Bouzid et al. 2022). To overcome these matrix effects, the use of PSF as internal standard was tested; once this polymer exhibited similar properties to those of PSLMW and PSHMW against different matrices. The effect of different matrices on $R_{D/T}$ was similar throughout the experiments performed with different polymers and methods of preparation, i.e., liquid solution of PSLMW and PSF or solid dilution of PSHMW. Therefore, the normalization of the analytes surface areas by those from PSF markers reduced the differences in the slopes of the calibration curves built in different matrices. This was only achieved when the corresponding fluoride marker was used, what is aligned with the principles of ISTD use, including sharing similar chromatographic properties (Unice, Kreider, and Panko 2012; Zhou, Yang, and Wang 2017).

An overall reduced formation of the three monitored pyrolysates was observed for PSLMW compared to PSHMW, leading to a considerable mass deficit. This might be attributed to the generation of other compounds unscreened for. For example, unsaturated compounds and heavier pyrolysates, i.e., oligomers with more than three repeating units, which are hardly analyzed by the common chromatographic-MS technique, might be preferably formed with the decreasing Mw (Costa and Camino 1982; Bouster, Vermande, and Veron 1989). Reduced yields of styrene dimer and trimer, to a negligible level, were also already observed for nanoplastics compared to microplastic, indicating a different formation or pyrolyzates from the microscale to the nanoscale (Blancho et al. 2021). The relative yields of PS markers significantly differed in the polymers with different Mw, notably the $R_{D/T}$, attributed to the higher quantity of dimer formed during the PSHMW pyrolysis. The thermo-degradation (or pyrolysis) of polymers are believed to follow a radical-based reaction, initiating mainly by random or end chain scission and forming macroradicals as stable as possible (Zhou et al. 2016; Duan et al. 2021). The initiation through chain-end scission might be particularly important with the decreasing of the Mw and the consequent increase in chain-end positions (Faravelli et al. 2001). The increase in chain-end positions in PSLMW, and likely the prevalence of an initiation reaction though chain-end scission, might play a role in the propagation reaction, thus privileging the formation of other markers instead of the dimer.

The formation of pyrolysates depends upon the microstructure of the polymer and the particle and on the relative bond strengths (Bouster, Vermande, and Veron 1989; Sam 2019; Park and Lee 2021; Miller et al. 2022). Changes in the aliphatic backbone of polymers as consequence of the weathering of microplastic in the environment, through mechanisms of chain scission and oxidation (Gewert, Plassmann, and MacLeod 2015;

Cai et al. 2018; Liu et al. 2021), might result in a lower Mw than the pristine microplastics used to build calibration curves. In this study, we present that such differences between the Mw led to quantification errors up to 5-fold, depending on the marker chosen. The consequences of the differences in polymer microstructure, such as degree of branching or cross-linking, on the quantification of polystyrene and other microplastics using pyr-GC-MS, remain to be investigated.

The PSHMW was insoluble in the solvents tested, likely due to its high Mw as the solubility and rate of dissolution of polymers are known to decrease with increasing molecular chains (Chojnacka, Janssen, and Schoenmakers 2014). Therefore, microplastic particles of PSHMW were added to solid matrices, which were mixed and milled. For the comparison with PSLMW, the same procedure was repeated for this polymer; i.e., microplastic particles of a similar size distribution were added to sand and submitted to several milling processes. The heterogeneity of solid samples prepared through a milling and mixing method directly affect the deviation among triplicates and the linearity of the curves, as observed in this study, which are considerably lower than those obtained in solution. It is worth noting that the mechanical and visco-elastic properties of polymers usually rise with increasing Mw (Balani et al. 2015), likely representing a higher inhomogeneity of PSHMW compared to PSLMW samples. However, the relative standard deviations between replicates and slopes of the curves were similar between these two polymer types. For the purposes of this study, the differences observed between the slopes of curves and the differences in the pyrolysates yields obtained from the two polymers highlight the relevance of Mw differences in the quantification of microplastics. For studies aiming the quantification of microplastics in environmental samples, it is important to reduce the uncertainties related with calibration curves by performing the standard-addition method (Rodriguez et al. 1995; Cimetiere et al. 2013) or improving the sample preparation procedure.

The direct analysis of spiked soils using pyr-GC-MS, without further pretreatment besides drying, sieving, and griding, allowed the detection of PS in a concentration above 0.25 g kg^{-1}, which was already reported in environmental samples, such as biosolids (Okoffo et al. 2020; Ainali et al. 2021b; Zhang et al. 2022). Nevertheless, this limit of detection remains considerably high and might be even higher for polymers which generates hundreds markers of similar intensity, such as polypropylene and polyethylene (Tsuge, Ohtani, and Watanabe 2011; La Nasa et al. 2020). A direct analysis of complex matrices, rich in organic and inorganic components, might affect the method repeatability due to the overload of undesirable constituents. Due to the limited amount of sample possible to be injected into the pyr-GC-MS, sample homogeneity is an important aspect (Dierkes et al. 2019; Steinmetz et al. 2020). Improving sample clean-up or preconcentration through enzymatic and chemical digestion, density separation, or applying pressurized liquid extraction, has been already proposed to increase the sensibility and/or remove matrices interferences (Fischer and Scholz-Böttcher 2017; Okoffo et al. 2020; Thomas et al. 2020). In some instances, the treatment of the sample was insufficient to eliminate this matrix effect (Bouzid et al. 2022), highlighting the importance of elucidating matrix effect previously to microplastic quantification. We argue that the well-known advantages of pyrolysis techniques, such as the minimal sample preparation, may be further explored to increase the sample purification. For example, the

application of multiple heating steps on each sample could allow the discrimination of the thermolabile natural organic matter previously to the pyrolysis of microplastics (Quénéa et al. 2006; Terán, Gonzalez-Vila, and Gonzalez-Perez 2009; Okoffo et al. 2020; La Nasa et al. 2021) and potentially contributing to higher sensitivity of microplastic detection in complex soil matrices.

Conclusion

A robust quantification of PS using pyr-GC-MS through external calibration curves must include the elucidation of potential matrix effects, circumventing them by the use of an internal standard, and the use of a reference standard that shares a similar Mw range. Without prior knowledge of the Mw, efforts must be made to estimate quantification errors and incorporate measurement uncertainties. In most cases, an underestimation of microplastic concentration is expected, given the potential weathering of the plastic found in the environment, which encompass molecular chain scission and, consequently, reduced Mw. The formation of styrene-trimer was less affected when pyrolyzing PS of different Mw and this marker is, therefore, recommended for the quantification of PS microplastic in samples. Finally, the direct analysis of soils enriched with PS, without any pretreatment, resulted in the detection of PS markers at concentrations already observed in the environment. However, further sample preparation efforts are needed to improve the robustness and sensitivity of microplastic quantification using pyr-GC-MS

Acknowledgments

We are grateful for the precious support of Amélie Macon and Marylou Volontier in the laboratory and to the two anonymous reviewers.

Disclosure statement

There are no relevant financial or non-financial competing interests to report.

Funding

This work was supported by the ISITE-BFC (Initiatives Science Innovation Territoire Economie en Bourgogne-Franche-Comté) through the SENSAAS (SENSors and Analyses for AquiferS) ISITE-BFC project (grant number: FC21010.CHR.IS - SENSAAS)

References

Ainali, N. M., D. N. Bikiaris, and D. A. Lambropoulou. 2021a. Aging effects on low- and high-density polyethylene, polypropylene and polystyrene under UV irradiation: An insight into decomposition mechanism by Py-GC/MS for microplastic analysis. *Journal of Analytical and Applied Pyrolysis*.158:105207. doi:10.1016/j.jaap.2021.105207.

Ainali, N. M., D. Kalaronis, A. Kontogiannis, E. Evgenidou, G. Z. Kyzas, X. Yang, D. N. Bikiaris, and D. A. Lambropoulou. 2021b. Microplastics in the environment: Sampling, pretreatment, analysis and occurrence based on current and newly-exploited chromatographic approaches. *The Science of the Total Environment* 794:148725. doi:10.1016/j.scitotenv.2021.148725.

Audisio, G., and F. Bertini. 1992. Molecular weight and pyrolysis products distribution of polymers I. *Journal of Analytical and Applied Pyrolysis* 24 (1):61–74. doi:10.1016/0165-2370(92)80005-7.

Balani, K., V. Verma, A. Agarwal, and R. Narayan. 2015. *Physical, thermal, and mechanical properties of polymers in biosurfaces: A materials science and engineering perspective*, 1st ed., 329–44. John Wiley Sons Inc.

Q1

Blancho, F., M. Davranche, H. E. Hadri, B. Grassl, and J. Gigault. 2021. Nanoplastics identification in complex environmental matrices: Strategies for polystyrene and polypropylene. *Environmental Science & Technology* 55 (13):8753–9. doi:10.1021/acs.est.1c01351.

Bouster, C., P. Vermande, and J. Veron. 1989. Evolution of the product yield with temperature and molecular weight in the pyrolysis of polystyrene. *Journal of Analytical and Applied Pyrolysis.*15:249–59. doi:10.1016/0165-2370(89)85038-7.

Bouzid, N., C. Anquetil, R. Dris, J. Gasperi, B. Tassin, and S. Derenne. 2022. Quantification of microplastics by pyrolysis coupled with gas chromatography and mass spectrometry in sediments: Challenges and implications. *Microplastics* 1 (2):229–39. doi:10.3390/microplastics1020016.

Bu, H., P. Yuan, H. Liu, D. Liu, J. Liu, H. He, J. Zhou, H. Song, and Z. Li. 2017. Effects of complexation between organic matter (OM) and clay mineral on OM pyrolysis. *Geochimica Et Cosmochimica Acta.*212:1–15. doi:10.1016/j.gca.2017.04.045.

Cai, L., J. Wang, J. Peng, Z. Wu, and X. Tan. 2018. Observation of the degradation of three types of plastic pellets exposed to UV irradiation in three different environments. *The Science of the Total Environment* 628-629:740–7. doi:10.1016/j.scitotenv.2018.02.079.

Chojnacka, A., H.-G. Janssen, and P. Schoenmakers. 2014. Detailed study of polystyrene solubility using pyrolysis–gas chromatography–mass spectrometry and combination with size-exclusion chromatography. *Analytical and Bioanalytical Chemistry* 406 (2):459–65. doi:10.1007/s00216-013-7461-5.

Cimetiere, N., I. Soutrel, M. Lemasle, A. Laplanche, and A. Crocq. 2013. Standard addition method for the determination of pharmaceutical residues in drinking water by SPE–L. *Environmental Technology*. 34:12.

Camino, G., L. Costa, and L. Trossarelli. 1982. Thermal degradation of polymer-fire retardant mixtures: Part VII–products of degradation and mechanism of fire retardance in polystyrene-chloroparaflin mixtures. *Polymer Degradation and Stability*. 4 (1):39–49. doi:10.1016/0141-3910(82)90004-0.

Dierkes, G., T. Lauschke, S. Becher, H. Schumacher, C. Földi, and T. Ternes. 2019. Quantification of microplastics in environmental samples via pressurized liquid extraction and pyrolysis-gas chromatography. *Analytical and Bioanalytical Chemistry* 411 (26):6959–68. doi:10.1007/s00216-019-02066-9.

Duan, J., N. Bolan, Y. Li, S. Ding, T. Atugoda, M. Vithanage, B. Sarkar, D. C. W. Tsang, and M. B. Kirkham. 2021. Weathering of microplastics and interaction with other coexisting constituents in terrestrial and aquatic environments. *Water Research* 196:117011. doi:10.1016/j.watres.2021.117011.

Dümichen, E., A.-K. Barthel, U. Braun, C. G. Bannick, K. Brand, M. Jekel, and R. Senz. 2015. Analysis of polyethylene microplastics in environmental samples, using a thermal decomposition method. *Water Research* 85:451–7. doi:10.1016/j.watres.2015.09.002.

Dümichen, E., P. Eisentraut, C. G. Bannick, A.-K. Barthel, R. Senz, and U. Braun. 2017. Fast identification of microplastics in complex environmental samples by a thermal degradation method. *Chemosphere* 174:572–84. doi:10.1016/j.chemosphere.2017.02.010.

Dziwiński, E. J., J. Iłowska, and J. Gniady. 2018. Py-GC/MS analyses of poly(ethylene terephthalate) film without and with the presence of tetramethylammonium acetate reagent. Comparative study. *Polymer Testing*. 65:111–5. doi:10.1016/j.polymertesting.2017.11.009.

Fabbri, D., C. Trombini, and I. Vassura. 1998. Analysis of polystyrene in polluted sediments by pyrolysis–gas chromatography–mass spectrometry. *Journal of Chromatographic Science*. 36 (12):600–4. doi:10.1093/chromsci/36.12.600.

Faravelli, T., M. Pinciroli, F. Pisano, G. Bozzano, M. Dente, and E. Ranzi. 2001. Thermal degradation of polystyrene. *Journal of Analytical and Applied Pyrolysis*.60 (1):103–21. doi:10.1016/S0165-2370(00)00159-5.

Faure, P., L. Schlepp, L. Mansuy-Huault, M. Elie, E. Jardé, and M. Pelletier. 2006. Aromatization of organic matter induced by the presence of clays during flash pyrolysis-gas chromatography–mass spectrometry (PyGC–MS). *Journal of Analytical and Applied Pyrolysis*.75 (1):1–10. doi:10.1016/j.jaap.2005.02.004.

Fischer, M., and B. M. Scholz-Böttcher. 2017. Simultaneous trace identification and quantification of common types of microplastics in environmental samples by pyrolysis-gas chromatography–mass spectrometry. *Environmental Science & Technology* 51 (9):5052–60. doi:10.1021/acs.est.6b06362.

Fischer, M., and B. M. Scholz-Böttcher. 2019. Microplastics analysis in environmental samples – recent pyrolysis-gas chromatography-mass spectrometry method improvements to increase the reliability of mass-related data. *Analytical Methods* 11 (18):2489–97. doi:10.1039/C9AY00600A.

Gewert, B., M. M. Plassmann, and M. MacLeod. 2015. Pathways for degradation of plastic polymers floating in the marine environment. *Environmental Science. Processes & Impacts* 17 (9):1513–21. doi:10.1039/c5em00207a.

Guigue, J., O. Mathieu, J. Lévêque, S. Mounier, R. Laffont, P. A. Maron, N. Navarro, C. Chateau, P. Amiotte-Suchet, and Y. Lucas. 2014. A comparison of extraction procedures for water-extractable organic matter in soils: Comparison of WEOM extraction procedures. *European Journal of Soil Science* 65 (4):520–30. doi:10.1111/ejss.12156.

Guo, D., S. Wu, G. Lyu, and H. Guo. 2017. Effect of molecular weight on the pyrolysis characteristics of alkali lignin. *Fuel* 193:45–53. doi:10.1016/j.fuel.2016.12.042.

ter Halle, A., L. Ladirat, M. Martignac, A. F. Mingotaud, O. Boyron, and E. Perez. 2017. To what extent are microplastics from the open ocean weathered? *Environmental Pollution (Barking, Essex: 1987)* 227:167–74. doi:10.1016/j.envpol.2017.04.051.

Hempfling, R., and H.-R. Schulten. 1990. Chemical characterization of the organic matter in forest soils by Curie point pyrolysis-GC/MS and pyrolysis-field ionization mass spectrometry. *Organic Geochemistry*. 15 (2):131–45. doi:10.1016/0146-6380(90)90078-E.

Huang, J., H. Chen, Y. Zheng, Y. Yang, Y. Zhang, and B. Gao. 2021. Microplastic pollution in soils and groundwater: Characteristics, analytical methods and impacts. *Chemical Engineering Journal and the Biochemical Engineering Journal*. 425:131870. doi:10.1016/j.cej.2021.131870.

Hurley, R. R., and L. Nizzetto. 2018. Fate and occurrence of micro(nano)plastics in soils: Knowledge gaps and possible risks. *Current Opinion in Environmental Science & Health*.1:6–11. doi:10.1016/j.coesh.2017.10.006.

IUPAC. 1997. *Compendium of chemical terminology (the "Gold Book")*. 2nd ed. Oxford: Blackwell Scientific Publications.

Käppler, A., D. Fischer, S. Oberbeckmann, G. Schernewski, M. Labrenz, K.-J. Eichhorn, and B. Voit. 2016. Analysis of environmental microplastics by vibrational microspectroscopy: FTIR, Raman or both? *Analytical and Bioanalytical Chemistry* 408 (29):8377–91. doi:10.1007/s00216-016-9956-3.

La Nasa, J., G. Biale, D. Fabbri, and F. Modugno. 2020. A review on challenges and developments of analytical pyrolysis and other thermo-analytical techniques for the quali-quantitative determination of microplastics. *Journal of Analytical and Applied Pyrolysis*.149:104841. doi:10.1016/j.jaap.2020.104841.

La Nasa, J., G. Biale, M. Mattonai, and F. Modugno. 2021. Microwave-assisted solvent extraction and double-shot analytical pyrolysis for the quali-quantitation of plasticizers and microplastics in beach sand samples. *Journal of Hazardous Materials* 401:123287. doi:10.1016/j.jhazmat.2020.123287.

Lauschke, T., G. Dierkes, P. Schweyen, and T. A. Ternes. 2021. Evaluation of poly(styrene-d5) and poly(4-fluorostyrene) as internal standards for microplastics quantification by thermoanalytical methods. *Journal of Analytical and Applied Pyrolysis*.159:105310. doi:10.1016/j.jaap.2021.105310.

Lenth, R. V., B. Bolker, P. Buerkner, I. Giné-Vázquez, M. Herve, M. Jung, J. Love, F. Miguez, H. Riebl, and H. Singmann. 2023. emmeans: Estimated Marginal Means, aka Least-Squares Means.

Leslie, H. A., M. J. M. van Velzen, S. H. Brandsma, A. D. Vethaak, J. J. Garcia-Vallejo, and M. H. Lamoree. 2022. Discovery and quantification of plastic particle pollution in human blood. *Environment International* 163:107199. doi:10.1016/j.envint.2022.107199.

Liu, X., P. Sun, G. Qu, J. Jing, T. Zhang, H. Shi, and Y. Zhao. 2021. Insight into the characteristics and sorption behaviors of aged polystyrene microplastics through three type of accelerated oxidation processes. *Journal of Hazardous Materials* 407:124836. doi:10.1016/j.jhazmat.2020.124836.

Miller, J. V., J. R. Maskrey, K. Chan, and K. M. Unice. 2022. Pyrolysis-gas chromatography-mass spectrometry (Py-GC-MS) quantification of tire and road wear particles (TRWP) in environmental matrices: Assessing the importance of microstructure in instrument calibration protocols. *Analytical Letters*. 55 (6):1004–16. doi:10.1080/00032719.2021.1979994.

Ogle, D. H., J. C. Doll, and A. P. Wheeler. 2023. (Provided base functionality of dunnTest). FSA: Simple Fisheries Stock Assessment Methods.

Ohtani, H., T. Yuyama, S. Tsuge, B. Plage, and H.-R. Schulten. 1990. Study on thermal degradation of polystyrenes by pyrolysis-gas chromatography and pyrolysis-field ionization mass spectrometry. *European Polymer Journal*. 26 (8):893–9. doi:10.1016/0014-3057(90)90164-Y.

Okoffo, E. D., F. Ribeiro, J. W. O'Brien, S. O'Brien, B. J. Tscharke, M. Gallen, S. Samanipour, J. F. Mueller, and K. V. Thomas. 2020. Identification and quantification of selected plastics in biosolids by pressurized liquid extraction combined with double-shot pyrolysis gas chromatography–mass spectrometry. *The Science of the Total Environment* 715:136924. doi:10.1016/j.scitotenv.2020.136924.

Park, C., and J. Lee. 2021. Pyrolysis of polypropylene for production of FUEL-RANGE products: Effect of molecular weight of polypropylene. *International Journal of Energy Research* 45 (9): 13088–97. doi:10.1002/er.6635.

Peñalver, R., N. Arroyo-Manzanares, I. López-García, and M. Hernández-Córdoba. 2020. An overview of microplastics characterization by thermal analysis. *Chemosphere* 242:125170. doi: 10.1016/j.chemosphere.2019.125170.

Picó, Y., and D. Barceló. 2020. Pyrolysis gas chromatography-mass spectrometry in environmental analysis: Focus on organic matter and microplastics. *TrAC Trends in Analytical Chemistry* 130:115964. doi:10.1016/j.trac.2020.115964.

Pinto da Costa, J., A. Paço, P. S. M. Santos, A. C. Duarte, and T. Rocha-Santos. 2019. Microplastics in soils: Assessment, analytics and risks. *Environmental Chemistry* 16 (1):18–30. doi:10.1071/EN18150.

PlasticsEurope. 2020. PlasticsEurope - The Facts 2020. Accessed June 17, 2021. https://www.plasticseurope.org/fr/resources/publications/1804-plastics-facts-2019.

Quénéa, K., S. Derenne, F. J. González-Vila, J. A. González-Pérez, A. Mariotti, and C. Largeau. 2006. Double-shot pyrolysis of the non-hydrolysable organic fraction isolated from a sandy forest soil (Landes de Gascogne, South-West France). *Journal of Analytical and Applied Pyrolysis*.76 (1-2):271–9. doi:10.1016/j.jaap.2005.12.007.

R Core Team. 2022. R: A Language and Environment for Statistical Computing (v 4.2.2), http://www.R-project.org/.

Renner, G., T. C. Schmidt, and J. Schram. 2018. Analytical methodologies for monitoring micro(-nano)plastics: Which are fit for purpose? *Current Opinion in Environmental Science & Health*.1:55–61. doi:10.1016/j.coesh.2017.11.001.

Ribeiro, F., E. D. Okoffo, J. W. O'Brien, S. Fraissinet-Tachet, S. O'Brien, M. Gallen, S. Samanipour, S. Kaserzon, J. F. Mueller, T. Galloway, et al. 2020. Quantitative analysis of selected plastics in high-commercial-value australian seafood by pyrolysis gas chromatography mass spectrometry. *Environmental Science & Technology* 54 (15):9408–17. doi:10.1021/acs.est.0c02337.

Rødland, E. S., E. D. Okoffo, C. Rauert, L. S. Heier, O. C. Lind, M. Reid, K. V. Thomas, and S. Meland. 2020. Road de-icing salt: Assessment of a potential new source and pathway of microplastics particles from roads. *The Science of the Total Environment* 738:139352. doi:10.1016/j.scitotenv.2020.139352.

Rodriguez, L. C., A. M. G. Campana, F. A. Barrero, C. J. Linares, and M. Roman. 1995. Validation of an analytical instrumental method by standard addition methodology. *Journal of AOAC INTERNATIONAL* 78 (2):471–6. doi:10.1093/jaoac/78.2.471.

Saiz-Jimenez, C., and J. W. De Leeuw. 1986. Chemical characterization of soil organic matter fractions by analytical pyrolysis-gas chromatography-mass spectrometry. *Journal of Analytical and Applied Pyrolysis.*9 (2):99–119. doi:10.1016/0165-2370(86)85002-1.

Sam, K. D. 2019. *Pyrolysis–gas chromatography in encyclopedia of analytical science*, eds. Worsfold, P., A. Townshend, C. Poole, and M. Miró. 3rd ed. Elsevier.

Q2

Scherer, C., A. Weber, F. Stock, S. Vurusic, H. Egerci, C. Kochleus, N. Arendt, C. Foeldi, G. Dierkes, M. Wagner, et al. 2020. Comparative assessment of microplastics in water and sediment of a large European river. *The Science of the Total Environment* 738:139866. doi:10.1016/j.scitotenv.2020.139866.

Steinmetz, Z., A. Kintzi, K. Muñoz, and G. E. Schaumann. 2020. A simple method for the selective quantification of polyethylene, polypropylene, and polystyrene plastic debris in soil by pyrolysis-gas chromatography/mass spectrometry. *Journal of Analytical and Applied Pyrolysis.*147: 104803. doi:10.1016/j.jaap.2020.104803.

Terán, A., F. J. Gonzalez-Vila, and J. A. Gonzalez-Perez. 2009. Detection of organic contamination in sediments by double-shoot pyrolysis–GC/MS. *Environmental Chemistry Letters* 7 (4): 301–8. doi:10.1007/s10311-008-0169-7.

Thomas, D., B. Schütze, W. M. Heinze, and Z. Steinmetz. 2020. Sample preparation techniques for the analysis of microplastics in soil—A review. *Sustainability* 12 (21):9074. doi:10.3390/su12219074.

Toapanta, T., E. D. Okoffo, S. Ede, S. O'Brien, S. D. Burrows, F. Ribeiro, M. Gallen, J. Colwell, A. K. Whittaker, S. Kaserzon, et al. 2021. Influence of surface oxidation on the quantification of polypropylene microplastics by pyrolysis gas chromatography mass spectrometry. *The Science of the Total Environment* 796:148835. doi:10.1016/j.scitotenv.2021.148835.

Tsuge, S., H. Ohtani, and C. Watanabe. 2011. *Pyrolysis - GC/MS data book of synthetic polymers* - 1st Edition.

Q3

Unice, K. M., M. L. Kreider, and J. M. Panko. 2012. Use of a deuterated internal standard with pyrolysis-GC/MS dimeric marker analysis to quantify tire tread particles in the environment. *International Journal of Environmental Research and Public Health* 9 (11):4033–55. doi:10.3390/ijerph9114033.

Veerasingam, S., M. Ranjani, R. Venkatachalapathy, A. Bagaev, V. Mukhanov, D. Litvinyuk, M. Mugilarasan, K. Gurumoorthi, L. Guganathan, V. M. Aboobacker, et al. 2021. Contributions of Fourier transform infrared spectroscopy in microplastic pollution research: A review. *Critical Reviews in Environmental Science and Technology* 51 (22):2681–743. doi:10.1080/10643389.2020.1807450.

Q4

Velimirovic, M., K. Tirez, S. Voorspoels, and F. Vanhaecke. 2021. Recent developments in mass spectrometry for the characterization of micro- and nanoscale plastic debris in the environment. *Analytical and Bioanalytical Chemistry* 413 (1):7–15. doi:10.1007/s00216-020-02898-w.

Wickham, H., W. Chang, L. Henry, T. L. Pedersen, K. Takahashi, C. Wilke, K. Woo, H. Yutani, and D. Dunnington. 2023. Posit, and PBC ggplot2: Create Elegant Data Visualisations Using the Grammar of Graphics.

Yakovenko, N., A. Carvalho, and A. ter Halle. 2020. Emerging use thermo-analytical method coupled with mass spectrometry for the quantification of micro(nano)plastics in environmental samples. *TrAC Trends in Analytical Chemistry* 131:115979. doi:10.1016/j.trac.2020.115979.

Zhang, J., S. Ren, W. Xu, C. Liang, J. Li, H. Zhang, Y. Li, X. Liu, D. L. Jones, D. Chadwick, et al. 2022. Effects of plastic residues and microplastics on soil ecosystems: A global meta-analysis. *Journal of Hazardous Materials* 435:129065. doi:10.1016/j.jhazmat.2022.129065.

Zhou, J., Y. Qiao, W. Wang, E. Leng, J. Huang, Y. Yu, and M. Xu. 2016. Formation of styrene monomer, dimer and trimer in the primary volatiles produced from polystyrene pyrolysis in a wire-mesh reactor. *Fuel* 182:333–9. doi:10.1016/j.fuel.2016.05.123.

Zhou, W., S. Yang, and P. G. Wang. 2017. Matrix effects and application of matrix effect factor. *Bioanalysis* 9 (23):1839–44. doi:10.4155/bio-2017-0214.